MICROSTRUCTURE - TOUGHNESS RELATIONSHIPS IN A C-Mn WELD METAL

J.H. Tweed and J.F. Knott*

A model is proposed for the cleavage failure of a C-Mn weld metal close to its transition temperature. The model involves strain-induced cracking of non-metallic inclusions to give cleavage nuclei, which then propagate under a critical tensile stress. The importance of inclusion size, chemistry, and associated tessellated stress fields is discussed.

INTRODUCTION

Carbon-manganese (C-Mn) weld metals are currently used in large quantities for offshore construction in the North Sea and elsewhere. For successful operation under such rigorous conditions, it is essential to achieve adequate weld-metal toughness at temperatures down to -10°C, or even lower. In particular, failure by cleavage, which gives rise to low fracture-toughness values, must be avoided. This paper presents an investigation of the role of the microstructure of a weld-metal in determining its susceptibility to cleavage and hence its fracture toughness.

Development of Microstructure

The microstructure of carbon-manganese weld-metals is complex. For a specified chemistry, the major factors determining the final microstructure are: the large, columnar, prior-austenite grains; a rapid cooling rate; and a relatively high volume fraction of fine deoxidation products (non-metallic inclusions). On cooling, equiaxed ferrite grains nucleate and grow from prior-austenite grain boundaries (grain-boundary ferrite). This is followed by the intragranular, inclusion-assisted, nucleation of fine acicular ferrite (Figure 1). Finally, carbon-enriched regions between the acicular ferrite laths, or adjacent to the grain boundary ferrite, may either transform to ferrite-carbide aggregates or martensite, or may remain, untransformed,as retained austenite (microphases). Possible transformation products are more fully described by Abson and Dolby (1), and Cochrane (2).

* Department of Metallurgy & Materials Science, University of Cambridge.

EXPERIMENTAL

Welding

The microstructure of manual-metal-arc welds consists of regions of as-deposited weld-metal, together with regions which have been recrystallised by succeeding weld beads. The British Standard for crack opening displacement (COD) fracture toughness testing (3) recommends that weld-metal toughness should be assessed using specimens of full plate thickness, with through-thickness fatigue pre-cracks. Hence, the fatigue pre-crack tip samples regions of as-deposited and recrystallised weld-metal. In the present experiments, a weldment was designed with a large central weld bead such that the tip of a pre-crack grown from the weld surface would lie wholly in as-deposited weld metal.

The welding was carried out by B.O.C. Murex using Ferex 7018LT electrodes on 25mm base plate conforming to British Standard 4360, Grade 50D. The large central bead was laid down using an 8mm electrode at a heat input of 4.2kJ mm^{-1}. The weldment was not restrained. Details of the weld are given by Tweed and Knott (4), whilst the chemical compositions of the weld-metal and base-plate are presented in Table 1.

TABLE 1 - Chemical Compositions of Weld-Metal and Base-Plate

Material	Composition in weight %							
	C	Mn	Si	S	P	Nb	Al	N
Base-Plate	0.16	1.55	0.29	0.011	0.017	0.047	0.010	0.008
Weld-metal	0.06	1.15	0.53	0.010	0.019	0.004	<0.005	0.014

Mechanical Testing

Crack opening displacement specimens of cross-section 10mm by 20mm were extracted from the weldment and tested generally according to B.S. 5762 (3). However it should be emphasised that the fatigue pre-cracks were grown from the weld surface so that the crack tip lay along the direction of welding. Three tests were performed at each of three temperatures (22°C, 0°C, -40°C). Corresponding tensile tests were carried out on Hounsfield Number 11 specimens with a gauge diameter of 3.1mm but with a shortened gauge length of 5.0mm, to ensure that the gauge length lay entirely within the large as-deposited weld bead. All tests were performed on a screw-driven, 50kN capacity, Mand testing machine operating at a cross-head displacement rate of 1mm min^{-1}.

Metallography

Fracture surfaces were examined using an ISI 100A scanning electron microscope (SEM) operated at 20kV, together with a Link Systems energy dispersive system for analysis of X-rays. Selected specimens were sectioned, etched, and examined optically. Quantitative microstructural information was obtained using a Quantimet 720 automatic image-analysing computer.

RESULTS

Mechanical Testing

The results of the tensile tests and the COD tests are presented in

Table 2. The COD specimens tested at -40°C failed by cleavage with no prior ductile crack growth. All other COD specimens failed by cleavage after some ductile crack growth. Although the COD values at 22°C are, on average, almost an order-of-magnitude greater than those at -40°C, the individual values at both temperatures vary by as much as a factor of three.

TABLE 2 - Mechanical Test Results

Temperature (°C)	-40	0	22
Yield Stress (MNm^{-2})	581	544	511
Tensile Stress (MNm^{-2})	687	643	591
Work-Hardening Exponent		0.125	
COD values (μm)	11, 24, 40	59, 65, 67	103, 148, 319

Metallography

The microhardnesses of the grain-boundary ferrite and acicular ferrite are 218 and 243 respectively. On yielding, deformation is localized, initially, in the grain-boundary ferrite.

Cleavage initiation sites were sought on fracture surfaces by following diverging river lines back to their source. Figure 2 shows a typical situation, in which the specimen failed at a COD of 11μm at -40°C. The tip of the fatigue pre-crack is indicated by the dotted line. River lines radiate from the site of a non-metallic inclusion (arrowed). A portion of the inclusion is present on each half of the fracture surface, indicating that the inclusion has cracked. The X-ray spectrum from this inclusion is shown in Figure 3(a). The large iron peaks are due to excitation of the matrix. Some initiating inclusions also show a major calcium peak and a minor potassium peak (Figure 3(b)).

The microstructure on a plane, polished and etched, section consists of 22% grain boundary ferrite. However, coarse facets, typically associated with grain boundary ferrite (4), occupy 40% of a fracture surface in the same orientation. This implies that cleavage propagates preferentially through grain-boundary ferrite.

Inclusion Characterization

The inclusion size distribution measured on a microvoided fracture surface is shown in Figure 4. Widgery and Knott (5) have suggested that an inclusion will be present on a microvoid-coalescence fracture surface if its distance from the average crack path is some simple, direct function of its diameter. A microvoid fracture surface inclusion distribution will thus emphasise the upper end of the size range.

A separate investigation was made of cracked inclusions on a microvoided fracture surface broken at 22°C. The size and chemistry of six such inclusions is indicated by the open symbols on Figure 4. (The chemical symbols are those of the major constituents). The full symbols on Figure 4 show the size and chemistry of five inclusions which were found to have initiated local cleavage failure at -40°C. Inclusions from the bulk of the microvoid fracture-surface distribution are high in manganese and silicon but the largest inclusions also contain calcium and some potassium. Cracked inclusions qualitatively exhibit

a chemistry typical of their size.

DISCUSSION

Two major qualitative models have been proposed to explain the toughness of C-Mn weld-metals. That due to Dolby (6) considers a competition between the volume fraction of the tougher acicular ferrite and the concomitant strength increase. High toughness is deduced for a low strength microstructure with no acicular ferrite, or a high strength microstructure containing little grain boundary ferrite. The model of Garland and Kirkwood (7) considers several other factors which may influence strength and toughness levels, and they propose that brittle fracture nucleation may occur at martensitic microphases, which are hence deleterious to toughness.

In addition to these two models, Billy et al. (8) and Farrar et al. (9) have proposed that carbides may act as brittle fracture nucleation sites, particularly after stress-relieving, during which carbides may coarsen.

Proposed Model

A model for the cleavage fracture of C-Mn weld metals has been proposed by the present authors (4). This involves initial plasticity in grain-boundary ferrite and plasticity-assisted inclusion fracture, followed by propagation of cleavage from these cracked inclusion nuclei preferentially through grain boundary ferrite. Various aspects of this model will be considered below.

Plasticity-Assisted Inclusion Fracture. Fractographic evidence (4) suggests that cleavage propagates from cracked inclusion nuclei. By analogy with models for propagation-controlled fracture in wrought mild steel (e.g. Smith (10)) it was assumed that this should occur at low matrix strains. However, inclusions on a microvoid-coalescence fracture surface have been subjected to high matrix strains, and the proportion of cracked inclusions on such a fracture surface is low (<1%) although their size and chemistry are generally typical of the bulk of the (fracture surface) inclusion distribution (Figure 4). Two unusually large inclusions, with significant calcium and potassium contents were both cracked. Thus, even with high matrix strains, few inclusions crack, though the large, calcium rich, inclusions are particularly susceptible. A critical combination of stress and strain may thus be required for inclusion fracture.

Inclusion nucleated cleavage. In this limited investigation five cases of inclusion-nucleated cleavage were positively identified (as in Figures 2 and 4). All initiating inclusions were approximately 1μm in diameter or larger. The two largest examples were calcium-rich. Initiating inclusions thus come from the top 10% of the inclusion distribution as presented in Figure 4 and it should be emphasised that the sampling method used for Figure 4 favours the upper end of the size distribution. It is thus expected that initiating inclusions represent the largest 2-5% of the bulk inclusion distribution.

Correlation of crack tip stresses with predicted failure stresses. If application of a Smith-type model is valid, there should be a reasonable correlation between the stress required to propagate a circular micro-crack of the inclusion diameter into the ferrite matrix, and the stress present at the inclusion site from the fatigue-crack-tip stress-field. Figure 2 is from a specimen which failed at a COD of 11μm at -40°C. The initiating inclusion is found at a distance of approximately twice the COD from the crack tip. This is the distance calculated by Rice and Johnson (11) for the maximum in the crack tip stress distribution. The stress required to propagate a circular crack of

radius a into the ferrite matrix is:

$$\sigma_F = \frac{\pi}{2}\left\{\frac{2E\gamma_p}{\pi(1-\nu^2)a}\right\}^{\frac{1}{2}}$$

In this case the initiating inclusion is 1μm in diameter giving a predicted fracture stress of 3100 MNm^{-2} if γ_p is taken as 14 Jm^{-2} (12). Assuming plane strain conditions the maximum stress ahead of a crack in a material with a work-hardening exponent of 0.125 is estimated from (11) to be $4.0\sigma_y$. McMeeking (13) suggests that this may be conservative by 6-8%. The maximum crack-tip stress may thus be as high as $4.3\sigma_y$; in this case 2500 MNm^{-2}. As the inclusion size increases the predicted fracture stress falls and, for these conditions, lies below the maximim crack-tip stress for inclusion diameters greater than 1.6μm. However, for inclusions between 1μm and 1.6μm in diameter, the crack-tip stresses should be insufficient to cause failure.

Influence of inclusion tessellated stress field. Manganese silicate inclusions contract less than ferrite on cooling. Hence, there will be a tessellated stress field in and around such inclusions. Brooksbank and Andrews (14) have shown that this consists of a hydrostatic compressive stress in the inclusion, coupled with compressive radial, and tensile circumferential stresses in the matrix. This latter stress will aid crack propagation. Its maximum value occurs at the inclusion-matrix interface, when the matrix is about to yield, and is of magnitude $\sigma_y/3$. This will have a small influence on the predicted fracture stress.

CONCLUSIONS

Further evidence has been presented to support a model for the cleavage fracture of C-Mn weld metals in which microcrack nuclei are formed by the fracture of inclusions. The largest of these nuclei propagate under the applied stress field. Occasional large calcium-manganese silicates are susceptible to cracking and may then give propagation at relatively low applied stresses. A discrepancy between the applied stress and the predicted failure stress for small nuclei may be partially reconciled by the presence of tessellated stress fields around the inclusions.

SYMBOLS USED

σ_y = yield stress (MNm^{-2})

σ_F = fracture stress (MNm^{-2})

E = Young's modulus for ferrite (200 GNm^{-2})

γ_p = effective surface energy for ferrite (14 Jm^{-2})

a = radius of cracked inclusion

ACKNOWLEDGEMENTS

The authors would like to thank Professor R.W.K. Honeycombe F.R.S., Goldsmith's Professor of Metallurgy, for provision of research facilities, B.O.C. Murex for provision of materials, and the Northern Ireland Department of Education for a maintenance grant for J.H.T.

REFERENCES

1. Abson, D.J., and Dolby, R.E., 1980, IIW Doc IXJ-29-80.
2. Cochrane, R.C., 1977, BSC Report T/PDM/462/1/77/C.
3. British Standards Institution, 1979, B.S. 5762: 1979.
4. Tweed, J.H., and Knott, J.F., Met. Sci., in press.
5. Widgery, D.J., and Knott, J.F., 1978, Met. Sci., 12, 8.
6. Dolby, R.E., 1976, Weld. Inst. Report R/RB/M93/76.
7. Garland, J.G., and Kirkwood, P.R., 1975, Met. Constr., 7, 275, 320.
8. Billy, J., Johansson, T., Loberg, B., and Easterling, K.E., 1980, Met. Tech., 7, 67.
9. Farrar, R.A., Taylor, L.G., and Harrison, E.M., 1979, Met. Tech., 6, 380.
10. Smith, E., 1968, Int. J. Fract. Mech., 4, 131.
11. Rice, J.R., and Johnson, M.A., 1970, Inelastic Behaviour of Solids, McGraw Hill, New York, 641.
12. Curry, D.A. and Knott, J.F., 1978, Met. Sci., 12, 511.
13. McMeeking, R.M., 1977, J. Mech. Phys. Solids, 25, 357.
14. Brooksbank, D., and Andrews, K.W., 1972, J.I.S.I., 210, 246.

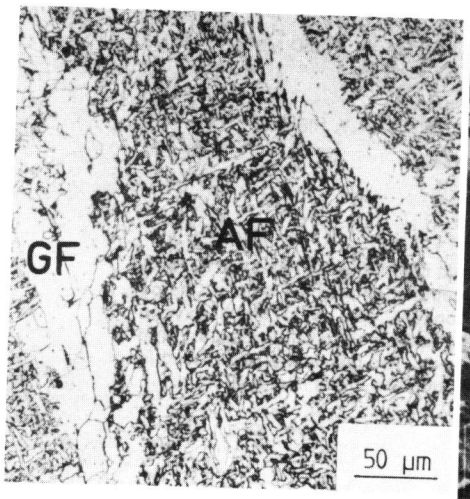

G F Grain Boundary Ferrite
A F Acicular Ferrite

Figure 1 Weld Microstructure

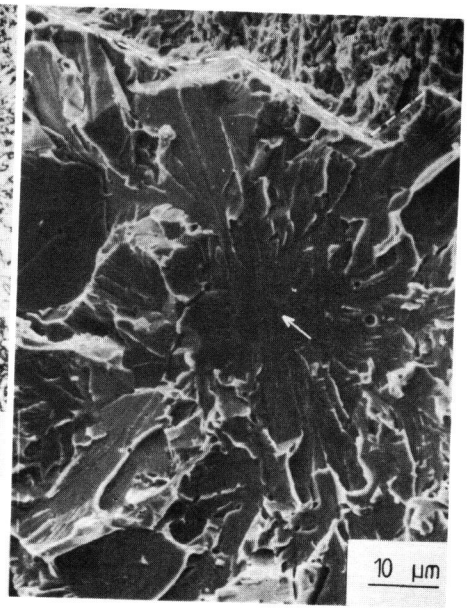

Figure 2 Cleavage Initiation Site

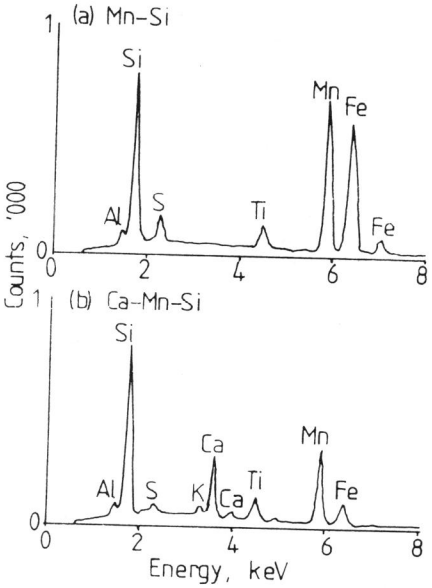

Figure 3 Typical Inclusion X-ray spectra

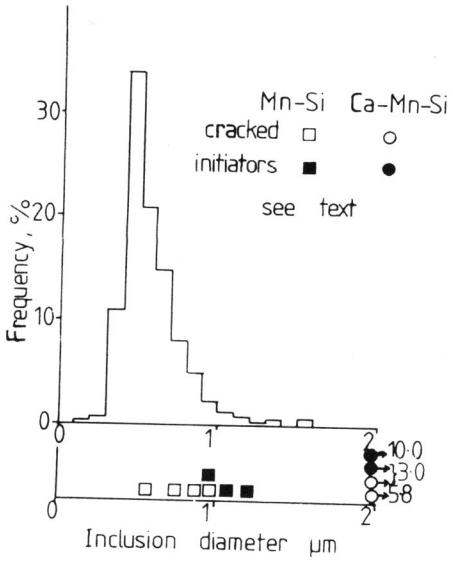

Figure 4 Inclusion size distributions